This paper is available online at www.jbc.org

THE JOURNAL OF BIOLOGICAL CHEMISTRY VOL. 285, NO. 13, pp. 9322–9326, March 26, 2010


# Recognition of Histone H3K4 Trimethylation by the Plant Homeodomain of PHF2 Modulates Histone Demethylation*[S]

Received for publication, December 21, 2009, and in revised form, January 13, 2010
Published, JBC Papers in Press, February 2, 2010, DOI 10.1074/jbc.C109.097667

**Hong Wen[‡§¶1], Jingzhi Li[‖1], Tanjing Song[‡§¶1], Ming Lu[‡], Pu-Yeh Kan[§**], Min Gyu Lee[§**], Bingdong Sha[‖], and Xiaobing Shi[‡§¶‡‡2]**

*From the Departments of [‡]Biochemistry and Molecular Biology and [**]Molecular and Cellular Oncology, the Centers for [§]Cancer Epigenetics and [¶]Stem Cell and Developmental Biology, and the [‡‡]Genes and Development Graduate Program, The University of Texas M. D. Anderson Cancer Center, Houston, Texas 77030 and the [‖]Department of Cell Biology, University of Alabama at Birmingham, Birmingham, Alabama 35205*

**Distinct lysine methylation marks on histones create dynamic signatures deciphered by the "effector" modules, although the underlying mechanisms remain unclear. We identified the plant homeodomain- and Jumonji C domain-containing protein PHF2 as a novel histone H3K9 demethylase. We show in biochemical and crystallographic analyses that PHF2 recognizes histone H3K4 trimethylation through its plant homeodomain finger and that this interaction is essential for PHF2 occupancy and H3K9 demethylation at rDNA promoters. Our study provides molecular insights into the mechanism by which distinct effector domains within a protein cooperatively modulate the "cross-talk" of histone modifications.**

Covalent post-translational modifications on histones play an essential role in regulating chromatin dynamics that influences diverse nuclear processes such as transcription (1–3). Methylation on distinct histone lysine residues is in general associated with different transcriptional states. For instance, methylation on H3K4 (H3K4me) is enriched in the regions of active transcription, whereas H3K9me is linked to transcriptional repression (4, 5). One of the fundamental mechanisms by which histone methylation regulates chromatin is to create dynamic signatures at chromatin that are recognized by "effector" proteins, which in turn transduce the chromatin signatures to downstream biological functions (6, 7). In this context, the plant homeodomains (PHD[3] fingers) from ING2 and BPTF have been shown to recognize H3K4me3 and subsequently regulate transcription (8, 9).

There are >200 PHD fingers in the human genome; however, the functions of most PHD fingers are not clear. Interestingly, a subfamily of PHD finger proteins also contain a JmjC domain, a recently identified module responsible for histone lysine demethylation (10–12), indicating that these PHD fingers may play a role in methylation dynamics. Therefore, we sought to determine whether the PHD fingers in the JmjC domain-containing KDM (lysine demethylase) proteins directly recognize histone methyllysines and whether they can modulate JmjC domain-dependent histone demethylation. In this study, we identified PHF2 (PHD finger protein 2) as a novel histone H3K9 demethylase, and we found that the PHF2 PHD finger specifically recognizes H3K4me3. We determined the crystal structure of the PHF2 PHD finger in complex with an H3K4me3 peptide and identified essential resides for this interaction. Finally, we demonstrate that recognition of H3K4me3 is important for PHF2-dependent promoter demethylation and expression of rDNA.

## EXPERIMENTAL PROCEDURES

*Plasmids, Antibodies, and Peptides*—The PHF2 PHD finger (residues 1–70) was cloned into pGEX-6P-1 (GE Healthcare). Mouse *phf2* cDNA was cloned into pENTR3C and subsequently cloned into the pDEST53, p3FLAG, and pBABE-FLAG vectors using Gateway techniques (Invitrogen). PHD mutants were generated by site-direct mutagenesis (Stratagene). Anti-PHF2 antibody (D45A2) was obtained from Cell Signaling. Anti-histone antibodies were from Abcam (H3 (Ab1791), H3K4me1 (Ab8895), H3K4me2 (Ab32356), H3K4me3 (Ab8580), H3K9me1 (Ab9045), H3K9me3 (Ab8898), H3K36me1 (Ab9048), H3K36me3 (Ab9050), H4K20me1 (Ab9051), H4K20me2 (Ab9052), and H4K20me3 (Ab9053)) or Upstate (H3K9me2 (07-441), H3K27me1 (07-448), H3K27me2 (07-452), H3K27me3 (07-449), and H3K36me2 (07-369)). Other antibodies used in this study were raised against fibrillarin (Ab5821, Abcam), GST (E5, Santa Cruz Biotechnology), and FLAG (M2) and tubulin (Sigma). Histone peptides bearing different modifications were synthesized at the W. M. Keck Facility at Yale University.

*Peptide Microarray and Peptide Pulldown Assays*—Peptide microarray and peptide pulldown assays were performed as described previously (13, 14). Briefly, biotinylated histone peptides were printed in hexaplicates onto a streptavidin-coated slide (Arrayit Corp.) using a VersArray compact microarrayer (Bio-Rad). After a short blocking with biotin (Sigma), the slides were incubated overnight at 4 °C with the GST-fused PHF2 PHD finger in binding buffer (50 mM Tris-HCl (pH 7.5), 300 mM NaCl, and 0.1% Nonidet P-40). After washing with the same

* This work was supported by Welch Foundation Grant G1719 and institutional research grants from the American Cancer Society and The University of Texas M. D. Anderson Cancer Center.

[S] The on-line version of this article (available at http://www.jbc.org) contains supplemental Figs. 1–7.

*The atomic coordinates and structure factors (code 3KQI) have been deposited in the Protein Data Bank, Research Collaboratory for Structural Bioinformatics, Rutgers University, New Brunswick, NJ (http://www.rcsb.org/).*

[1] These authors contributed equally to this work.

[2] To whom correspondence should be addressed: Dept. of Biochemistry and Molecular Biology, The University of Texas M. D. Anderson Cancer Center, 1515 Holcombe Blvd., Houston, TX 77030. Tel.: 713-834-6293; Fax: 713-792-0346; E-mail: xbshi@mdanderson.org.

[3] The abbreviations used are: PHD, plant homeodomain; BPTF, bromodomain PHD finger transcription factor; JmjC, Jumonji C; GST, glutathione *S*-transferase; MES, 4-morpholineethanesulfonic acid; shRNA, short hairpin RNA; ChIP, chromatin immunoprecipitation; WT, wild-type.

**TABLE 1**

**X-ray crystallographic data collection, phasing, and refinement statistics**

The highest resolution shell is shown in parentheses. Zn-SAD, zinc single-wavelength anomalous diffraction; r.m.s.d., root mean square deviation.

| | Native | Zn-SAD |
|---|---|---|
| **Data collection** | | |
| Space group | P6(5)22 | P6(5)22 |
| Cell dimensions | | |
| *a*, *b*, *c* (Å) | 77.76, 77.76, 72.12 | 77.93, 77.93, 72.07 |
| $\alpha$, $\beta$, $\gamma$ | 90°, 90°, 120° | 90°, 90°, 120° |
| Wavelength (Å) | 1.000 | 1.283 |
| Resolution (Å) | 30-1.78 (1.84-1.78) | 30-1.91 (1.94-1.91) |
| $R_{sym}$ or $R_{merge}$ | 7.0 (38.1) | 8.4 (42.3) |
| $I/\sigma I$ | 40.0 (3.8) | 66.9 (5.2) |
| Completeness (%) | 98.5 (89.1) | 98.0 (83.6) |
| Redundancy | 9.0 (4.8) | 19.9 (9.1) |
| **Refinement** | | |
| Resolution (Å) | 1.78 | |
| No. reflections | 11,858 | |
| $R_{work}/R_{free}$ | 18.9/21.8 | |
| No. atoms | | |
| Protein | 622 | |
| Ion | 6 | |
| Water | 125 | |
| *B*-factors | | |
| Protein | 30.4 | |
| Ion | 50.8 | |
| Water | 40.2 | |
| r.m.s.d. | | |
| Bond lengths (Å) | 0.009 | |
| Bond angles | 1.170° | |

buffer, slides were probed with anti-GST antibody and fluorescein-conjugated secondary antibody and visualized using a GenePix 4000 scanner (Molecular Devices). For peptide pulldown assays, 1 $\mu$g of biotinylated histone peptides with different modifications was incubated overnight with 1 $\mu$g of GST-fused PHD fingers in binding buffer. Streptavidin beads (Amersham Biosciences) were added to the mixture and incubated for 1 h with rotation. The beads were then washed three times and analyzed by SDS-PAGE and Western blotting.

*X-ray Crystallography*—The purified PHF2 PHD finger protein was mixed with H3K4me3 peptide at a 1:2 ratio in a solution of 10 mM Tris-HCl (pH 7.5), 200 mM NaCl, 0.3 M urea, and 0.2% Tween 20 to concentrate to 10 mg/ml. Crystals of the complex were obtained by the hanging-drop vapor diffusion method at room temperature. The well solution consisted of 1 ml of 100 mm MES (pH 6.0) and 1.8 M ammonium sulfate. The crystals were flash-frozen at 100 K in a nitrogen gas stream in the cryoprotectant with 20% ethylene glycol. Zinc single-wavelength anomalous diffraction data were collected at peak wavelength and processed using Denzo and Scalepack software. The data collection and refinement statistics are shown in Table 1. The two zinc positions in the protein were determined using SHELXD (15). The phases were calculated using the programs SOLVE and RESOLVE (16). The model was built using COOT7, and the structure was refined using REFMAC (CCP4 Suite) (17). Figures were generated using the PyMOL molecular viewer.

*Cell Culture and shRNA-mediated Knockdown*—293T, U2OS, and HeLa cells were maintained in Dulbecco's modified Eagle's medium supplemented with 10% fetal bovine serum (Invitrogen). HeLa cell lines stably expressing PHF2 were generated using retrovirus. To knock down PHF2, cells were transfected with pTRIPZ-PHF2 shRNA (Open Biosystems) for 24 h, followed by a second transfection for an additional 48 h. The mature sense sequence of shRNA targeting human PHF2 is 5′-GAAACTACTCCTTTAAGAT-3′.

*Immunostaining, PCR, and ChIP Assays*—Immunostaining (18), reverse transcription-PCR, real-time PCR, and ChIP assays were performed as described previously (19). mRNA was prepared using an RNeasy Plus kit (Qiagen) and reverse-transcribed using a first-strand synthesis kit (Invitrogen). Quantitative real-time reverse transcription-PCR was performed on an ABI PRISM 7700 sequence detection system using Power SYBR Green PCR Master Mix (Applied Biosystems). Gene expressions were calculated following normalization to glyceraldehyde-3-phosphate dehydrogenase levels by the comparative cycle threshold method. Primer sequences used for rDNA ChIP analyses were as described previously (20).[4]

## RESULTS AND DISCUSSION

*The PHF2 PHD Finger Binds to H3K4me2/3*—We and others have previously developed a histone peptide array for high-throughput screening of the methylated histone-binding activity of candidate proteins or domains (13, 14). In brief, we printed ~400 spots of nearly 70 histone peptides bearing different degrees or combinations of methylation, acetylation, and phosphorylation on distinct residues on a slide, followed by incubation with candidate proteins or domains. We probed the PHD fingers present in the JmjC family proteins with the peptide arrays, and we found that the PHD fingers from PHF2 family proteins (Fig. 1*A*) and the third PHD fingers from JARID1A (JmjC and ARID domain-containing protein 1A) and JARID1B bound to H3K4me2/3 (Fig. 1*B* and data not shown). The binding of H3K4me2/3 by these PHD fingers was prohibited by phosphorylation at $Thr^3$ but was not affected by acetylation at $Lys^9$ or $Lys^{14}$ on the same peptide, indicating that these PHD fingers may recognize only the first few residues of the histone H3 tail. Sequence alignment showed high homology between these domains and the ING2 and BPTF PHD fingers, two known H3K4me3 binders (supplemental Fig. 1*A*). To further confirm these bindings, we performed peptide pulldown assays with histone peptides bearing mono-, di-, or trimethylation at H3K4, H3K9, H3K27, H3K36, H3K79, or H4K20, and the results suggested that the binding of H3K4me2/3 by the PHD fingers is specific (Fig. 1*C* and data not shown).

*Crystal Structure of the PHF2 PHD-H3K4me3 Complex*—To understand the molecular basis of this recognition, we determined the structure of the PHF2 PHD-H3K4me3 complex by x-ray crystallography to 1.78-Å resolution (Fig. 1*D* and supplemental Fig. 1, *B* and *C*). The diffraction data and refinement statistics are shown in Table 1. The overall fold of the PHF2 PHD finger is similar to that of the ING2 and BPTF PHD fingers (supplemental Fig. 1, *D* and *E*) (21, 22). There are two antiparallel $\beta$-sheets in the core of the PHF2 PHD finger, and three short $\alpha$-strands swing at one side of the $\beta$-sheets. Similar to other PHD modules, the PHF2 PHD finger covers two zinc finger motifs: $His^{31}$ coordinates one zinc atom with $Cys^{31}$ and $Cys^{34}$, and $Cys^{23}$ and $Cys^{26}$ form the second zinc finger motif with C-50 and C-53. The H3K4me3 peptide interacts with the

[4] Other primer sequences are available upon request.

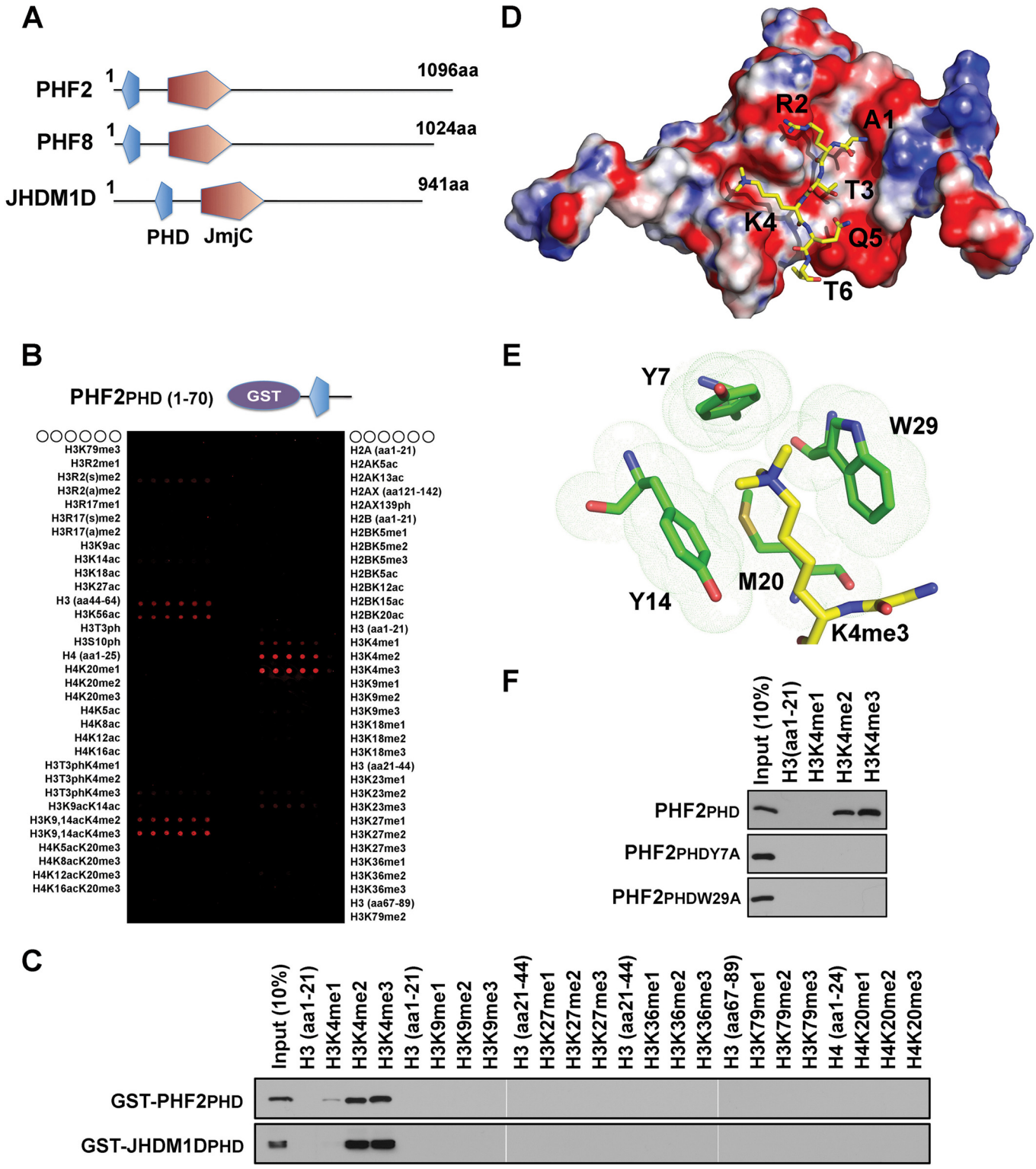


FIGURE 1. **The PHF2 PHD finger specifically binds to histone H3K4me2/3.** *A*, schematic representation of human PHF2 family proteins. *B*, the PHF2 PHD finger binds to H3K4me2/3 in a histone peptide array. Note that H3 (amino acids (*aa*) 44–64) peptides showed nonspecific binding. *C*, Western analysis of PHF2 and JHDM1D PHD fingers in peptide pulldown assays. *D*, crystal structure of the PHF2 PHD finger in complex with an H3K4me3 peptide. The PHD finger is shown as electrostatic surface, with *red* as negatively charged surface and *blue* as positively charged surface, and the histone peptide is shown as a stick, with carbon, oxygen, and nitrogen atoms colored *yellow*, *red*, and *blue*, respectively. *E*, stick representation of H3K4me3 (*yellow*) in the aromatic cage of the PHF2 PHD finger composed of $Tyr^{7}$, $Tyr^{14}$, $Met^{20}$, and $Trp^{29}$ residues (*green*). *D–E* were generated using PyMOL. *F*, Western analysis of peptide pulldown assays as described in *C* with PHF2 PHD finger mutants Y7A and W29A.

PHD finger through an antiparallel $\beta$-sheet pairing, and the side chains of $Arg^{2}$ and K4me3 of the histone H3 tail are positioned in two adjacent surface channels separated by a tryptophan residue of the PHD finger. Recognition of the trimethyl group by the PHF2 PHD finger is slightly different from that by the ING2 or BPTF PHD finger. The trimethyl ammonium group of $Lys^{4}$ is

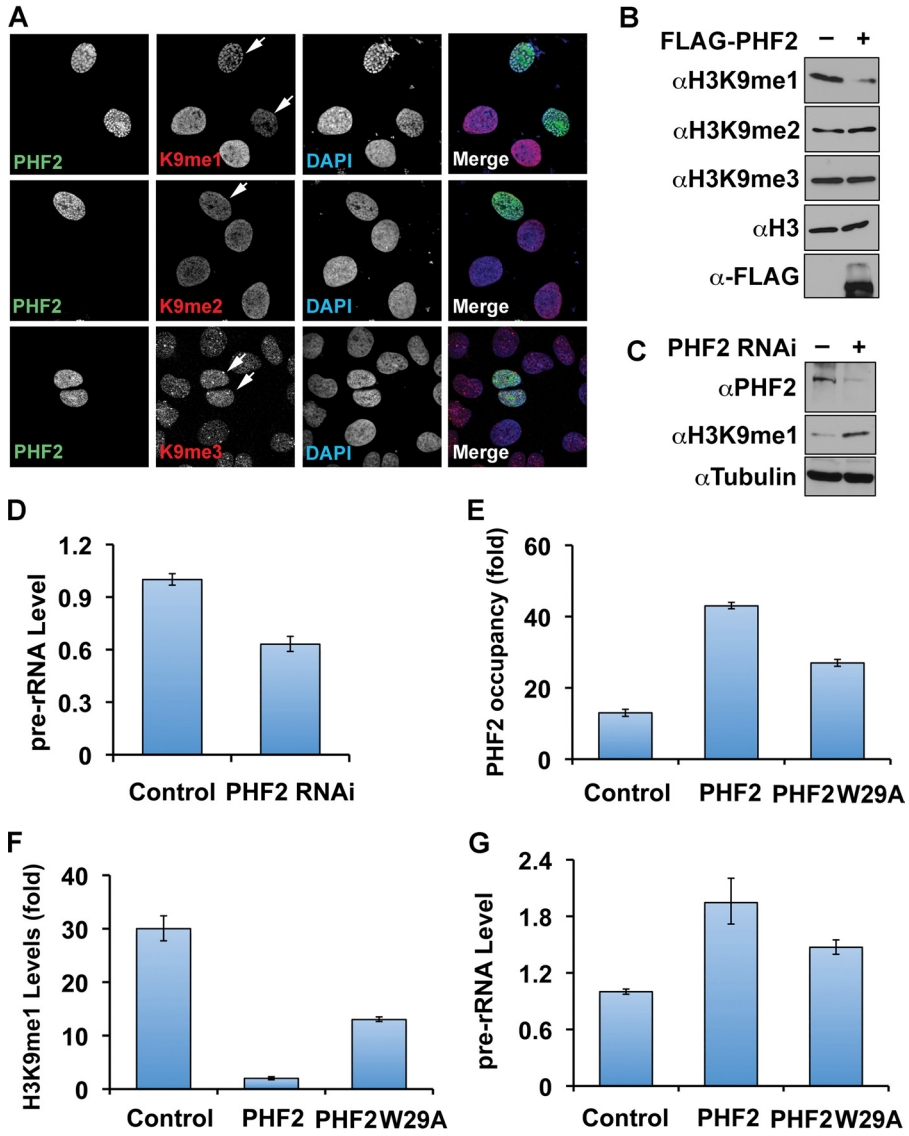


FIGURE 2. **The PHD finger is important for PHF2-mediated promoter demethylation and expression of rDNA.** *A* and *B*, PHF2 specifically demethylates H3K9me1 *in vivo*. *A*, immunostaining of U2OS cells expressing green fluorescent protein-tagged PHF2 with the indicated anti-H3K9me antibodies and 4′,6-diamidino-2-phenylindole (*DAPI*). Cells expressing ectopic PHF2 are indicated with *arrows*. *B*, Western analysis with the indicated antibodies of whole cell extracts from 293T cells transfected with FLAG-PHF2. Ectopic PHF2 was detected with anti-FLAG antibody. Histone H3 is shown as a loading control. *C*, knockdown of PHF2 increases the H3K9me1 level. Shown are the results from Western analysis performed with endogenous PHF2 and total H3K9me1 levels in whole cell extract from 293T cells expressing control or PHF2 shRNA. Tubulin is shown as a loading control. *RNAi*, RNA interference. *D*, knockdown of PHF2 decreases pre-rRNA levels. Shown are the results from real-time PCR analysis of pre-rRNA levels in 293T cells expressing control or PHF2 shRNA. *E*, the PHD finger is required for PHF2 occupancy at the rDNA promoter. Shown are the results from real-time PCR analysis of the rDNA promoter for PHF2 ChIP samples from cells expressing PHF2 or PHF2(W29A). ChIP signals are shown as -fold relative to IgG ChIPs. *F*, the PHD finger is required for PHF2-mediated H3K9 demethylation at the rDNA promoter. Shown are the results from real-time PCR analysis of the rDNA promoter for H3K9me1 ChIP samples as described for *E*. *G*, mutation in the PHD finger attenuates PHF2-dependent activation of rDNA expression. Shown are the results from real-time PCR analysis of pre-rRNA levels in 293T cells as in described for *E*. In *D–G*, *error bars* represent S.E., and all *p* values are $<0.05$.

stabilized by three aromatic residues ($Tyr^7$, $Tyr^{14}$, and $Trp^{29}$) in the PHF2 PHD finger, compared with two and four aromatic residues in the ING2 and BPTF PHD fingers, respectively (Fig. 1*E* and supplemental Fig. 1, *C* and *E*). As predicted, mutations targeting these residues disrupted H3K4me2/3 binding of the PHF2 PHD finger (Fig. 1*F*).

*PHF2 Is an H3K9me1-specific Histone Demethylase*—Phylogenetic analysis suggested that the JmjC domains in the PHF2 family are closely related to those in the JHDM1 (JmjC domain-containing histone demethylase 1) KDM group, yet their enzymatic activities have not been ascertained (10). To determine whether PHF2 is a functional KDM and which lysine residue(s) on histone proteins it demethylates, we overexpressed green fluorescent protein-tagged mouse PHF2 in U2OS cells and stained the cells with a variety of methylated histone-specific antibodies. We found that, *in vivo*, PHF2 specifically demethylated H3K9me1 but not H3K9me2 or H3K9me3 (Fig. 2*A*). In addition, PHF2 did not demethylate mono-, di-, or trimethylation at H3K4, H3K27, H3K36, or H4K20 (supplemental Figs. 2*A* and 3). We further confirmed the specificity of the H3K9me1 demethylation activity of PHF2 by Western analysis of whole cell extracts from 293T cells expressing ectopic PHF2 (Fig. 2*B*, supplemental Fig. 2*B*, and data not shown). Finally, we knocked down endogenous PHF2 and observed an increase in H3K9me1 levels in PHF2-depleted cells (Fig. 2*C*). Collectively, these data suggest that PHF2 specifically demethylates H3K9me1 *in vivo*.

Next, we asked whether the PHD finger is required for PHF2 demethylation activity. Although the W29A mutation abolished H3K4me2/3 binding of the PHF2 PHD finger *in vitro* (Fig. 1*F*), cells expressing the PHF2(W29A) mutant had similar H3K9me1 levels compared with cells expressing WT PHF2 (supplemental Fig. 4), indicating that the PHD finger may not be required for PHF2 demethylation activity *in vivo*, at least under overexpression condition. This does not exclude the requirement of the PHD finger for PHF2 demethylation at target chromatin loci because overexpression may drive PHF2 to chromatin regions at which PHF2 does not function under physiological conditions.

*PHF2 Regulates rRNA Expression in Nucleoli*—Immunostaining of endogenous PHF2 proteins in U2OS cells showed a co-localization of PHF2 with the nucleolar protein fibrillarin, and this was further confirmed by staining with antibody M2 in HeLa S3 cells stably expressing low levels of FLAG-PHF2 (supplemental Fig. 5). We therefore hypothesized that PHF2

might regulate rRNA expression in nucleoli. Indeed, compared with control cells, the pre-rRNA levels decreased in cells expressing PHF2 shRNA (Fig. 2*D*; see supplemental Fig. 6 for PHF2 knockdown efficiency). To further determine whether rRNA expression is directly regulated by PHF2, we performed ChIP analysis using the antibody against PHF2 protein. The ChIP results showed that endogenous PHF2 bound to rDNA promoter regions (supplemental Fig. 7), suggesting that PHF2 directly regulates rRNA expression. Notably, the occupancy of PHF2 on rDNA genes overlaps with H3K4me3: enriched at the promoter regions compared with the upstream, downstream, and coding regions (supplemental Fig. 7).

*The PHD Finger Is Required for PHF2-dependent Regulation of rRNA Expression*—To determine whether the recognition of H3K4me3 by the PHD finger is essential for PHF2 occupancy at rDNA promoters, we expressed WT PHF2 and the PHF2(W29A) mutant in cells for ChIP analysis. PHF2(W29A) occupancy at rDNA promoters was significantly reduced compared with that of ectopic WT PHF2 despite their similar expression levels (Fig. 2*E* and data not shown), suggesting that the H3K4me3-binding activity of the PHD finger is required for PHF2 occupancy at rDNA promoters. Consistent with this, the histone H3K9me1 level at rDNA promoters was significantly reduced in cells expressing WT PHF2 compared with that in control cells, whereas the reduction of H3K9me1 was compromised in cells expressing PHF2(W29A) (Fig. 2*F*). Finally, overexpression of PHF2, but not the PHF2(W29A) mutant, significantly increased pre-rRNA expression (Fig. 2*G*).

In this study, we identified a novel KDM, PHF2, that specifically demethylates H3K9me1, and we found that it recognizes another methyl mark, H3K4me3, through its PHD finger. Histone modifications play a complex role in the regulation of chromatin activities such as transcription. The histone modification cross-talk theory posits that one modification recruits histone-modifying complexes to modulate a second histone modification and that different modifications act in concert in these processes (6, 23, 24). In this context, the PHD fingers from ING2 and BPTF have been shown to recognize H3K4me3 at chromatin and help retain the ING2-histone deacetylase and BPTF-NURF complexes at the target promoter loci for subsequent histone deacetylation or chromatin remodeling by other enzymatic proteins in their complexes (8, 9). It was also shown that two domains, the Eaf3 chromodomain and the Rco1 PHD finger, in the same Rpd3S-histone deacetylase complex work combinatorially in recognizing H3K36me to facilitate histone deacetylation by Rpd3 at the transcribed regions in yeast (25). Here, we have shown that PHF2 contains two distinct domains (PHD and JmjC) within the same protein for the recognition of one methyl mark (H3K4me3) and removal of an opposite methyl mark (H3K9me1) and that recognition of H3K4me3 is essential for H3K9 demethylation at the proper chromatin loci. This might be a common mechanism for histone demethylation because many JmjC domain-containing KDM proteins contain PHD fingers and/or Tudor domains, another methyllysine-binding module (26). Interestingly, the JARID1A/B proteins contain PHD fingers and JmjC domains, both acting on the same modification (H3K4me3). Further characterization of these recognitions and enzymatic actions would be of great interest.

*Acknowledgments—We are indebted to O. Gozani and M. Bedford for scientific discussions. We thank M. Galko and X. Chen for critical reading of the manuscript and A. Kuo, R. Enlow, and Y. Yan for technical assistance.*

## REFERENCES

1. Berger, S. L. (2007) *Nature* **447,** 407–412
2. Kouzarides, T. (2007) *Cell* **128,** 693–705
3. Margueron, R., Trojer, P., and Reinberg, D. (2005) *Curr. Opin. Genet. Dev.* **15,** 163–176
4. Shilatifard, A. (2006) *Annu. Rev. Biochem.* **75,** 243–269
5. Li, B., Carey, M., and Workman, J. L. (2007) *Cell* **128,** 707–719
6. Jenuwein, T., and Allis, C. D. (2001) *Science* **293,** 1074–1080
7. Martin, C., and Zhang, Y. (2005) *Nat. Rev. Mol. Cell Biol.* **6,** 838–849
8. Shi, X., Hong, T., Walter, K. L., Ewalt, M., Michishita, E., Hung, T., Carney, D., Peña, P., Lan, F., Kaadige, M. R., Lacoste, N., Cayrou, C., Davrazou, F., Saha, A., Cairns, B. R., Ayer, D. E., Kutateladze, T. G., Shi, Y., Côté, J., Chua, K. F., and Gozani, O. (2006) *Nature* **442,** 96–99
9. Wysocka, J., Swigut, T., Xiao, H., Milne, T. A., Kwon, S. Y., Landry, J., Kauer, M., Tackett, A. J., Chait, B. T., Badenhorst, P., Wu, C., and Allis, C. D. (2006) *Nature* **442,** 86–90
10. Klose, R. J., Kallin, E. M., and Zhang, Y. (2006) *Nat. Rev. Genet.* **7,** 715–727
11. Shi, Y. (2007) *Nat. Rev. Genet.* **8,** 829–833
12. Agger, K., Christensen, J., Cloos, P. A., and Helin, K. (2008) *Curr. Opin. Genet. Dev.* **18,** 159–168
13. Shi, X., Kachirskaia, I., Walter, K. L., Kuo, J. H., Lake, A., Davrazou, F., Chan, S. M., Martin, D. G., Fingerman, I. M., Briggs, S. D., Howe, L., Utz, P. J., Kutateladze, T. G., Lugovskoy, A. A., Bedford, M. T., and Gozani, O. (2007) *J. Biol. Chem.* **282,** 2450–2455
14. Matthews, A. G., Kuo, A. J., Ramón-Maiques, S., Han, S., Champagne, K. S., Ivanov, D., Gallardo, M., Carney, D., Cheung, P., Ciccone, D. N., Walter, K. L., Utz, P. J., Shi, Y., Kutateladze, T. G., Yang, W., Gozani, O., and Oettinger, M. A. (2007) *Nature* **450,** 1106–1110
15. Schneider, T. R., and Sheldrick, G. M. (2002) *Acta Crystallogr. D Biol. Crystallogr.* **58,** 1772–1779
16. Terwilliger, T. C., and Berendzen, J. (1999) *Acta Crystallogr. D Biol. Crystallogr.* **55,** 849–861
17. Emsley, P., and Cowtan, K. (2004) *Acta Crystallogr. D Biol. Crystallogr.* **60,** 2126–2132
18. Wen, H., Andrejka, L., Ashton, J., Karess, R., and Lipsick, J. S. (2008) *Genes Dev.* **22,** 601–614
19. Shi, X., Kachirskaia, I., Yamaguchi, H., West, L. E., Wen, H., Wang, E. W., Dutta, S., Appella, E., and Gozani, O. (2007) *Mol. Cell* **27,** 636–646
20. Grandori, C., Gomez-Roman, N., Felton-Edkins, Z. A., Ngouenet, C., Galloway, D. A., Eisenman, R. N., and White, R. J. (2005) *Nat. Cell Biol.* **7,** 311–318
21. Peña, P. V., Davrazou, F., Shi, X., Walter, K. L., Verkhusha, V. V., Gozani, O., Zhao, R., and Kutateladze, T. G. (2006) *Nature* **442,** 100–103
22. Li, H., Ilin, S., Wang, W., Duncan, E. M., Wysocka, J., Allis, C. D., and Patel, D. J. (2006) *Nature* **442,** 91–95
23. Fischle, W., Wang, Y., and Allis, C. D. (2003) *Curr. Opin. Cell Biol.* **15,** 172–183
24. Latham, J. A., and Dent, S. Y. (2007) *Nat. Struct. Mol. Biol.* **14,** 1017–1024
25. Li, B., Gogol, M., Carey, M., Lee, D., Seidel, C., and Workman, J. L. (2007) *Science* **316,** 1050–1054
26. Huang, Y., Fang, J., Bedford, M. T., Zhang, Y., and Xu, R. M. (2006) *Science* **312,** 748–751